A target-selected *Apc*-mutant rat kindred enhances the modeling of familial human colon cancer

James M. Amos-Landgraf*, Lawrence N. Kwong*, Christina M. Kendziorski†, Mark Reichelderfer‡, Jose Torrealba§, Jamey Weichert¶, Jill D. Haag*, Kai-Shun Chen*, Jordy L. Waller*, Michael N. Gould*, and William F. Dove*‖**

Departments of †Biostatistics and Medical Informatics, §Pathology and Laboratory Medicine, ¶Radiology, and ‡Medicine, Section of Gastroenterology and Hepatology, *McArdle Laboratory for Cancer Research, and ‖Laboratory of Genetics, University of Wisconsin School of Medicine and Public Health, Madison, WI 53726

Contributed by William F. Dove, January 3, 2007 (sent for review December 19, 2006)

Progress toward the understanding and management of human colon cancer can be significantly advanced if appropriate experimental platforms become available. We have investigated whether a rat model carrying a knockout allele in the gatekeeper gene *Adenomatous polyposis coli* (*Apc*) recapitulates familial colon cancer of the human more closely than existing murine models. We have established a mutagen-induced nonsense allele of the rat *Apc* gene on an inbred F344/NTac (F344) genetic background. Carriers of this mutant allele develop multiple neoplasms with a distribution between the colon and small intestine that closely simulates that found in human familial adenomatous polyposis patients. To distinguish this phenotype from the predominantly small intestinal phenotype found in most *Apc*-mutant mouse strains, this strain has been designated the polyposis in the rat colon (Pirc) kindred. The Pirc rat kindred provides several unique and favorable features for the study of colon cancer. Tumor-bearing Pirc rats can live at least 17 months, carrying a significant colonic tumor burden. These tumors can be imaged both by micro computed tomography scanning and by classical endoscopy, enabling longitudinal studies of tumor genotype and phenotype as a function of response to chemopreventive and therapeutic regimes. The metacentric character of the rat karyotype, like that of the human and unlike the acrocentric mouse, has enabled us to demonstrate that the loss of the wild-type *Apc* allele in tumors does not involve chromosome loss. We believe that the Pirc rat kindred can address many of the current gaps in the modeling of human colon cancer.

chromosome biology | genomic instability | Min mouse | virtual colonoscopy | endoscopy

Colon cancer is a major cause of morbidity and mortality in the Western world: 148,610 new cases and 55,170 deaths are estimated for 2006 in the United States (1). Beyond early detection and surgical removal of the adenomatous precursor lesions, therapeutic approaches to colon cancer are currently inadequate.

The majority of human sporadic and familial adenomatous polyposis (FAP) colonic tumors involve mutations that inactivate the regulatory gene *APC*. Mouse strains carrying mutagen-induced or targeted mutations in the ortholog *Apc* develop intestinal adenomas. Thus, the *APC*/*Apc* gene has been designated a "gatekeeper" tumor-suppressor gene (2).

Most mouse strains mutated in *Apc*, including the Apc^{Min} (Min) strain, develop tumors primarily in the small intestine and die within several months from multiple such adenomas (3). Derivatives in which an *Apc* mutation is combined with mutations in the homeobox gene *Cdx2* (4) or the Tgfβ-signaling element *Smad3* (5) shift the proportion of tumors toward the colon. But the former construct creates a genomic instability and the phenotype of the latter construct seems to depend on a contribution from the commensal microbial flora, unlike the Min mouse (6).

Other platforms for the experimental investigation of colon cancer have their own limitations. Carcinogen-induced colonic neoplasms in the mouse and rat arise with a long latency at low multiplicity and incomplete penetrance. Models in which human tumors are xenografted into immunodeficient mice lack the microenvironment of the corresponding autochthonous tumor (7, 8). The deficiencies in modeling human colon cancer with animal and *in vitro* models have generated a challenge recently summarized by Sjoblom *et al.* (9): "For cancer biology, it is clear that no current animal or *in vitro* model of cancer recapitulates the genetic landscape of an actual human tumor."

The world of biomedical research on colon cancer is severely hampered by the lack of a reliable preclinical experimental platform. We have chosen to investigate whether a rat model carrying a knockout allele in *Apc* can simulate more closely the human disease. In pursuing this possibility, we have been emboldened by the newly developed ability to generate rat strains mutated in a gene of interest (10–13) and by the report that chemically induced colonic neoplasms in the rat can metastasize to distant sites such as the liver (14).

Our goals in seeking an enhanced experimental model for familial human colon cancer include the following: (*i*) to incorporate a dependence on a mutation in *Apc*, thus matching genetically the majority of FAP and sporadic colon cancers in the human; (*ii*) to simulate the regional distribution between the colon and small intestine of neoplasms found in the human; (*iii*) to enhance the probability of metastasis by enabling long lifespans and large tumor sizes; and (*iv*) to create a platform permitting prospective longitudinal studies with enhanced statistical power through imaging and endoscopy of long-lived animals with high tumor multiplicities. This report presents evidence that we have achieved important aspects of each of these goals.

Results

The Generation, Detection, and Molecular Characterization of a Rat Knockout Allele of *Apc*. To identify a founder for a mutant *Apc* rat kindred, we screened genomic DNA from 1,360 progeny of *N*-ethyl-*N*-nitrosourea (ENU)-treated males for truncating mutations in the *Apc* gene (Fig. 1*A*). A single male harbored a heterozygous point

Author contributions: J.M.A.-L. and L.N.K. contributed equally to this work; J.M.A.-L., L.N.K., J.D.H., M.N.G., and W.F.D. designed research; J.M.A.-L., L.N.K., M.R., J.W., J.D.H., and J.L.W. performed research; J.M.A.-L., L.N.K., C.M.K., J.D.H., and K.-S.C. contributed new reagents/analytic tools; J.M.A.-L., L.N.K., C.M.K., and J.T. analyzed data; and J.M.A.-L., L.N.K., and W.F.D. wrote the paper.

The authors declare no conflict of interest.

Freely available online through the PNAS open access option.

Abbreviations: CT, computed tomography; ENU, *N*-ethyl-*N*-nitrosourea; F344, F344/NTac; FAP, familial adenomatous polyposis; LOH, loss of heterozygosity; Min, Apc^{Min}; Pirc, polyposis in the rat colon; SNP, single nucleotide polymorphism; WF, Wistar Furth substrain WF/NHsd.

Data deposition: The sequence reported in this paper has been deposited in the Rat Genome Database (accession no. 1554322).

**To whom correspondence should be addressed at: McArdle Laboratory for Cancer Research, 1400 University Avenue, Madison, WI 53706. E-mail: dove@oncology.wisc.edu.

This article contains supporting information online at www.pnas.org/cgi/content/full/0611690104/DC1.

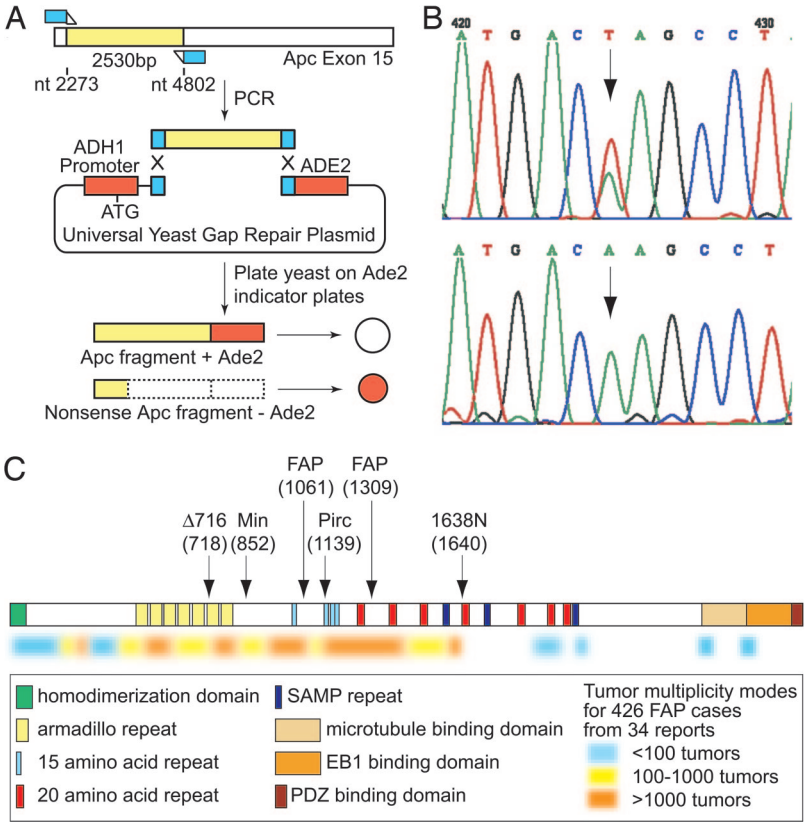

Fig. 1. Isolation and identification of the Pirc line of rats. (*A*) Scheme for the colorimetric yeast assay. Two thousand five hundred and thirty bases of *Apc* exon 15 spanning codons 757–1,600 were amplified with primers chimeric for *Apc* sequence and homology to a ''universal vector'' that accepts any such chimeric amplicon (11). The amplicon was then gap-repaired into the universal vector and transformed into ADE2-deficient yeast. Screening of 1,360 F1 progeny yielded a single yeast plate with half-red and half-white colonies, which is the expected ratio for a heterozygous mutant. (*B*) Sequence trace of the founder rat showing heterozygosity for the A→T transversion at nucleotide 3409 of *Apc* (*Upper*) compared with a wild-type littermate (*Lower*). (*C*) Structure of the human *Apc* gene. Arrows indicate orthologous locations of mouse model and Pirc truncating mutations and the two most common FAP mutation sites. The color bar below indicates the genotype–phenotype correlation of sites of protein truncation to disease severity.

mutation at nucleotide 3409 of *Apc*, creating a K.Xam (AAG.TAG) change at codon 1137 (Fig. 1*B*). No other mutations were found after sequencing the coding region and intron–exon junctions 5′ of the mutation. We therefore named this allele Apc^{am1137}. The predicted Apc protein would be truncated at the third amino acid of the second 15-aa β-catenin binding domain (Fig. 1*C*), which is highly conserved among vertebrates.

Neoplasms in Heterozygotes and Embryonic Lethality of Homozygotes for the Apc^{am1137} Allele. We analyzed the phenotype of F344-$Apc^{am1137/+}$ animals at the second and third backcross generations to F344. At ≈11 months of age, males became moribund from rectal bleeding, anemia, and weight loss. By contrast, females carrying this mutation have survived >17 months of age with no external signs of disease. Dissections at ages ranging from 88 to 397 days revealed multiple neoplasms in the intestinal tract of both male and female heterozygotes (Table 1). Importantly, extensive polyposis was observed in the colon, with a 100% incidence after 4 months of age. The strain was thus designated the F344-polyposis in the rat colon (Pirc) kindred.

Mutant rats in the F344-Pirc kindred also developed a number of microadenomas <0.5 mm in diameter in both the colon and small intestine (Table 1). Analysis of the molecular histopathology of polyps and microadenomas will be discussed below. Full necropsies of animals carrying the Apc^{am1137} mutation also uncovered tumors of the jaw in 6 of 10 long-lived females and benign epidermoid cysts in a majority of animals, but no overt distant metastases were uncovered.

The Pirc polyposis phenotype segregated perfectly with the Apc^{am1137} allele in 56 carriers and 23 noncarriers, supporting the hypothesis that this mutation causes the disease. There is less than a 5% chance that a separate mutation >3.8 cM from *Apc* would

Table 1. Tumor multiplicities in Pirc rats

Background	Sex	Age, months	No.	Colonic polyps, mean ± SD	Lesions in small intestine, mean ± SD	
					Adenomas	Microadenomas
F344-Pirc	Male	3	5	2 ± 1	7 ± 9	21 ± 20
	Male	4–6	10	8 ± 3	14 ± 5	88 ± 64
	Male	7–13	17	14 ± 8	22 ± 9	178 ± 116
	Female	3	5	3 ± 2	0 ± 0	1 ± 2
	Female	4–6	11	5 ± 3	2 ± 2	19 ± 29
	Female	7–13	6	7 ± 5	4 ± 5	35 ± 44
F344-Pirc, ENU-treated	Male	7	3	79 ± 11	57 ± 13	665 ± 103
F344-Pirc, mock-treated*	Male	7	2	11 ± 12	18 ± 8.5	208 ± 223

Colonic microadenoma multiplicities could not be accurately measured without histopathological confirmation and were excluded from these analyses. Neoplasms <0.5 mm in size were classified as microadenomas.
*Controls were injected with phosphocitrate buffer plus ethanol without ENU.

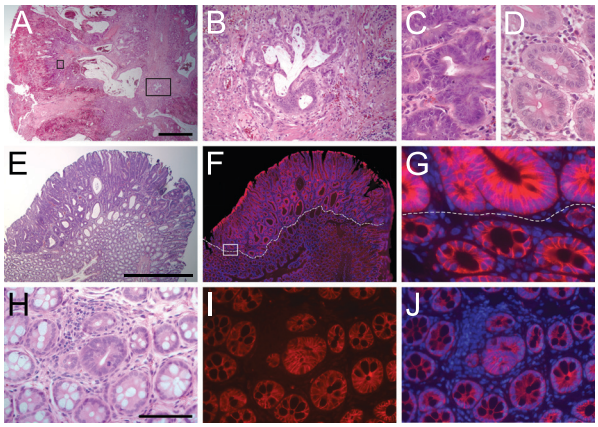

Fig. 2. Histological and gross appearance of Pirc tumors. (*A*) H&E of a focal adenocarcinoma with high-grade dysplasia. (*B*) Enlargement of the larger rectangle in *A*, showing invasion into the stalk. (*C* and *D*) Enlargement of the smaller rectangle in *A* (*C*), showing high-grade dysplasia compared with normal crypts from the same section (*D*). (*E*) H&E of a peduncular colonic adenoma. (*F*) β-catenin (red) and DAPI (blue) immunofluorescence of the same tumor. The dashed line delineates dysplastic (above the line) and hyperplastic and normal tissue (below the line). (*G*) Magnification of the rectangle shown in *F*. (*H*) H&E of a colonic microadenoma (central crypt) surrounded by normal crypts, which is representative of all colonic microadenomas examined. (*I*) β-catenin (red). (*J*) β-catenin (red) merged with DAPI (blue). (Scale bars: *A* and *E*, 1 mm; *H*, 0.1 mm.)

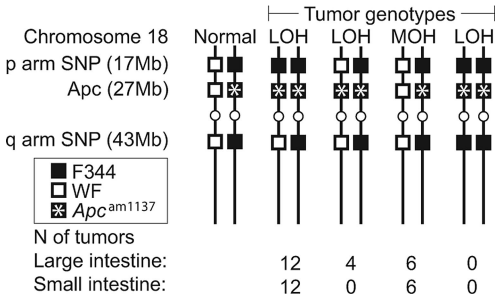

Fig. 3. LOH analysis for chromosome 18 on (F344xWF) F1 and F2 tumors. The three SNPs tested, ss48531311 (17 Mb) and *Apc*^{am1137} (27 Mb) on the p arm and ss48531727 (43 Mb) on the q arm, were all heterozygous in the normal tissue. The centromere (open circles) lies at approximately the 38-Mb position. LOH status at each SNP was determined by using a quantitative Pyrosequencing assay. Four possible tumor genotypes are given (left to right): LOH involving only the two loci on the p arm, LOH involving only *Apc*^{am1137}, maintenance of heterozygosity (MOH) at all three loci, and LOH for all three loci. We have diagrammed homozygosity; it must be noted that these Pyrosequencing assays cannot distinguish between hemizygosity (deletion) and homozygosity (recombination).

show this degree of association [see supporting information (SI) *Text*). No significant differences in the multiplicity or phenotype of intestinal tumors were seen between successive backcross generations of the F344-Pirc kindred on the inbred F344 background, indicating that any effect of ENU-induced modifying alleles is relatively minor.

We investigated whether the *Apc*^{am1137} mutation is homozygous-lethal by intercrossing *Apc*$^{am1137/+}$ animals on either an inbred F344 or a [F344 × WF/NHsd (WF)] F_1 background. No homozygous mutants were obtained of 71 total progeny, with heterozygotes and wild-type progeny exhibiting a 49:22 segregation, not significantly different from the expected 2:1 Mendelian ratio ($P > 0.8$, χ^2 test). Thus, the *Apc*^{am1137} allele is homozygous-lethal on two genetic backgrounds. In the formal possibility that this lethality is caused by a second ENU-induced mutation, it would lie within 2.4 cM (95% CI) of the *Apc*^{am1137} mutation (*SI Text*).

Age, Gender, and Carcinogen (ENU) Effects on the Pirc Phenotype. A significant dependence on gender was observed, with males developing more tumors throughout the intestinal tract. There was also a monotonic increase in tumor multiplicity with age, reaching an average of 14 colonic adenomas in males and 7 in females > 8 months of age (Table 1 and SI Table 4). The presence of colonic tumors in females at early ages, when tumors of the small intestine are not detected (Table 1), implies that colonic tumors arise first.

To increase the tumor multiplicity and consequent statistical power of the Pirc rat, male rats segregating the *Apc*^{am1137} allele were injected with a single dose of 40 mg/kg of ENU at 2 weeks of age. At 7 months of age, treated Pirc animals developed nearly 80 colonic tumors (Table 1) without major external signs of distress. This finding represents a 7-fold increase over mock-treated Pirc controls, whereas only a 3-fold increase was observed in macroadenomas of the small intestine. The wild-type littermate control rats receiving the same dose of ENU did not develop any detectable intestinal lesions. ENU-treated Pirc rats could therefore provide enhanced statistical power for experimental studies of chemopreventive and therapeutic regimens.

Long-Lived Pirc Animals Develop Adenocarcinomas with Local Invasion. The histopathology and morphology of the tumors closely resembled that of human tumors, with adenomatous changes evident, including dysplasia, nuclear enlargement, an increased mitotic rate, and the expansion of crypts showing loss of the normal columnar architecture (Fig. 2). Grossly, most colonic tumors were peduncular, whereas adenomas in the small intestine had a flat appearance. Each type of adenoma frequently reached 1 cm in diameter in animals over 6 months of age and up to 2 cm in those approaching 1 year. Immunofluorescent staining of tumors revealed nuclear and cytoplasmic accumulation of β-catenin within dysplastic cells (Fig. 2 *F* and *G*) as well as up-regulation of the proliferation marker Ki-67 (data not shown). By contrast, microadenomas of the colon and small intestine expressed Ki-67 but failed to show a convincing nuclear accumulation of β-catenin in any of >5,000 cells assayed (Fig. 2 *H–J* and data not shown). Longitudinal studies are needed to ascertain the neoplastic potential of these lesions. Importantly, in animals at 6 months of age or greater, 3 of 14 histologically examined colonic tumors were shown to have high-grade dysplasia accompanied by the local invasion of neoplastic cells into the stalk, classifying the tumors as adenocarcinomas with early signs of progression to a stage corresponding to T1 in the human (Fig. 2 *A–C*).

Loss of Heterozygosity at the *Apc*^{am1137} Site: Chromosome Loss Is Not Involved. Loss of heterozygosity (LOH) at the *Apc*^{am1137} site on the inbred F344 background was quantitatively assayed by using Pyrosequencing technology. Pyrosequencing is a registered trademark of Biotage (Uppsala, Sweden). Control assays of allele ratio were performed on DNA from normal intestinal tissue from *Apc*$^{am1137/+}$ heterozygotes. The allele ratios determined on tumor and control DNA were then plotted together and analyzed by a Gaussian mixture model (SI Fig. 5). The majority of F344 adenomas in the colon (87%, 34 of 39) and small intestine (100%, 24 of 24) showed LOH of the wild-type *Apc* allele at codon 1137.

Studies of LOH in the mouse face an obstacle in rigorously ascertaining chromosome loss with or without reduplication. The acrocentric character of the mouse karyotype prevents a systematic survey of both sides of the centromere. When LOH involves somatic recombination, only one arm of the chromosome is usually involved, in contrast to the chromosome-wide pattern found for chromosome-loss events. The rat karyotype is metacentric, by contrast, permitting us to test whether the LOH event observed in tumors involved whole-chromosome loss or loss followed by reduplication.

In F1 and F2 heterozygous animals (WF X F344)-*Apc*$^{am1137/+}$, we addressed whether the function of the wild-type WF allele of Apc

Table 2. The effect of celecoxib on the multiplicity of intestinal tumors >1 mm in diameter in F344 Pirc rats

Sex	Tissue	Tumor multiplicity, mean ± SD (no. of rats)		*P* value
		Treated	Untreated	
Male	Small intestine	1.3 ± 1.2 (12)	7.6 ± 4.3 (11)	<0.005
Male	Colon	1.2 ± 0.9 (12)	3.6 ± 2.7 (11)	<0.01
Female	Small intestine	0.8 ± 0.9 (12)	0.6 ± 0.8 (15)	0.6
Female	Colon	0.3 ± 0.5 (12)	1.3 ± 0.7 (15)	<0.001

Animals were treated from 40 days of age with 1,200 ppm celecoxib in Teklad 8604 chow and euthanized at 6–7 months of age. Tumors were counted on freshly dissected tissue without using a dissecting microscope. *P* values were determined by using the Wilcoxon rank sum test.

is lost through elimination of the entire WF chromosome. Polymorphic SNPs on the p and q arms of rat chromosome 18 were assayed in tumors and in adjacent normal, heterozygous tissue (Fig. 3). None of 22 colonic or 18 small intestinal tumors showed loss of both arms of the WF homolog. Rather, 16 colonic and 12 small intestinal tumors showed single-arm LOH, with all loss events involving the *Apc* locus on the p arm and often extending at least 10 Mb distal of *Apc*. Each case of LOH entailed loss of the WF allele and maintenance of the F344 allele. Thus, most tumors in the Pirc rat involve LOH at the Apc locus either by somatic recombination or by extended deletion. The remaining 12 tumors maintained heterozygosity over the entire chromosome 18. These tumors may have either silenced the wild-type *Apc* allele or inactivated it by an intragenic mutation (15, 16).

The Chemopreventive Action of Celecoxib. The Min mouse strain has enabled the analysis of the chemoprevention of intestinal adenomagenesis. The nonsteroidal antiinflammatory agents piroxicam (17), sulindac (18), and the clinically used celecoxib (19) have been reported to show significant efficacy in the Min mouse (for a review, see ref. 20). Statistically significant evidence for these effects depended on the high multiplicity of adenomas in the small intestine. By contrast, colonic tumor multiplicities in the range of two compromised the power of tests for an effect in the colon. Study designs involving large numbers of animals, enhanced colonic tumor multiplicities, or longitudinal analysis of individual imaged tumors would permit the analysis of response for colonic neoplasms.

The F344-Pirc rat kindred overcomes this obstacle. We have carried out an investigation of the action of celecoxib to prove this principle (Table 2). Treated mutant rats were fed celecoxib in their chow from 40 days of age and were killed at 6–7 months of age. Significant reductions in tumor multiplicity were found in the colon for both male and female rats and in the small intestine for males. Only a small number of tumors were found in the small intestine of females (also see Table 1), preventing a rigorous statistical analysis of this class of tumor.

The Rat Permits both Classical Endoscopy and Virtual Colonoscopy. To determine whether longitudinal *in vivo* studies of individual intestinal tumors can be carried out in trials with agents such as celecoxib, an 11-month-old F344-Pirc rat was anesthetized and its tumors visualized by endoscopy. As shown in Fig. 4*B*, a 6-mm-diameter bronchoscope provided clear images of three tumors with diameters 5.3, 5.7, and 6.8 mm. The same tumors were identified in three-dimensional micro computed tomography (CT) images (Fig. 4*A*) and confirmed upon dissection (Fig. 4*C*).

Discussion

It is widely believed that extant animal models of colon cancer do not fully recapitulate the human disease. Specifically, a major practical consideration is the lack of a significant colonic tumor burden for genetic, therapeutic, or diet studies. Either the abundance of small intestinal tumors prevents long-term analysis or the low absolute colonic tumor multiplicity hinders statistical analysis. In Table 3, we summarize the salient considerations in seeking an experimental model for human colon cancer. Importantly, the Pirc rat addresses several of the major drawbacks of all *Apc*-based models of familial intestinal cancer in the mouse.

One improvement is in the distribution of tumors in the intestinal tract. In measuring this component, we took into account the nuclear and cytoplasmic translocation of β-catenin, which is considered a hallmark of Apc-loss-associated neoplasia. Because no microadenomas showed such accumulation, only macroadenomas were considered. The ratio of macroadenoma multiplicities in the colon to that in the small intestine in Pirc rats averages 1:1. By contrast, most lines of C57BL/6-Min mice have an average ratio of ≈1:40. Although it is true that $Cdx2^{+/-}$ $Apc^{\Delta 716}$ mice have a 1:4 ratio (4), and $Smad3^{-/-}$ $Apc^{Min/+}$ mice develop polyps only in the colon (5), these models represent germline genotypes more complex than that of the FAP human. Furthermore, the short lifespans of both models make them less than ideal for chemopreventive studies. In comparing the mouse and rat with humans, it is important to note that human FAP patients do not develop polyps solely in the colon. Rather, the polyp incidence in the small intestine ranges from 58% to 74% at first endoscopy and approaches 100% by 70 years (21), with multiplicities exceeding 80 in 17% of patients monitored with video capsule endoscopy (22). Thus, the distribution of intestinal tumors in the Pirc rat resembles that in human FAP patients.

The Pirc rat also improves on another aspect: the absolute incidence and multiplicity of colonic tumors, which are higher in F344-Pirc rats than in carcinogen-treated wild-type F344 rats or in Min mice (Table 3). The ENU treatment of Pirc rats provides an even greater advantage in the statistical power of studies of chemopreventive and therapeutic protocols. Additionally, Pirc colonic tumors are capable of reaching a diameter in excess of 1 cm, enhancing the analysis of the volume and cellular composition of a tumor. Finally, the capacity for longitudinal studies in long-lived Pirc rats provides further qualitative advantages by using either specialized microCT instrumentation or, more generally, the clinical bronchoscope to bypass dissection as the necessary endpoint.

Our proof of principle of *in vivo* tumor imaging paves the way for investigation into the sensitivity and specificity of endoscopy versus

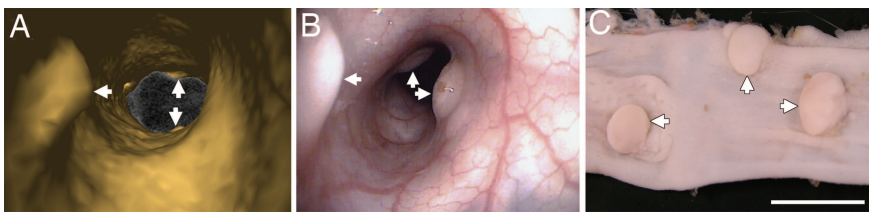

Fig. 4. *In vivo* imaging of Pirc tumors. MicroCT (*A*), endoscopic (*B*), and dissection (*C*) views of three colonic tumors in an 11-month-old F344 Pirc male. (Scale bar: 1 cm.)

Table 3. Comparison of FAP human, Min mouse, and Pirc rat colorectal cancer phenotypes.

Human FAP/animal model	Average colonic tumor count (age observed)	Average colonic tumor incidence, %	Average colonic: small intestinal tumor count ratio	Chromosomal organization
Human FAP (codon 700-1500)	>100 (>12 years)	100	>1:1	Metacentric
C57BL/6J-Min mouse (codon 850)	2–4 (>2 months)	40–80	<1:40	Acrocentric
F344 rat treated with carcinogen [typically β-catenin mutations (ref. 31)]	1–2 (>10 months)	80–90 (ref. 32)	0:1	Metacentric
F344-Pirc rat (codon 1137)	10 (>4 months)	100	1:1	Metacentric

Ranges are for strain averages, not for individual animals. The majority of data for carcinogen-treated rats uses time points later than 10 months of age.

virtual colonoscopy (23). Endoscopy also enhances the statistical power of pharmacologic and genetic investigations, minimizing the numbers of tumor-bearing rats required in these studies. We note with interest that the chemopreventive action of celecoxib is not complete (Table 3). Thus, such tumor resistance, as well as longitudinal studies of tumor progression, regression, and recurrence, can be related prospectively to molecular profiles of endoscopic biopsies. This ability to biopsy large tumors and allow the remaining portion to progress represents a unique opportunity unavailable in humans or in mice.

In addition to these physical advantages, the rat possesses at least one major genetic advantage: the metacentric rat karyotype permits a direct test of the mechanism of LOH that is unavailable in acrocentric mouse models. In future detailed studies of genomic stability versus instability during the initiation and progression of colonic neoplasms, the analysis will benefit significantly not only from the genetic homogeneity of inbred strains, but from the fact that the metacentric karyotype can distinguish between whole chromosome loss and somatic recombination or deletion *in vivo*.

Finally, the familial colonic tumors we have observed to date have progressed to locally invasive adenocarcinomas corresponding to human stage T1 lesions (Fig. 2 *A* and *B*). In developing the Pirc kindred in the rat, we are encouraged by the report of metastasis to the liver of chemically induced colonic adenocarcinomas in wild-type rats (14). We are also encouraged by the progress of the molecular genetics in the rat, including a rapidly closing genome project (24) and a growing set of genetic resources including large recombinant–inbred sets (25), transgenic strains, and ENU-induced mutant alleles in genes of interest (10, 12). Any of these resources could help fulfill the need for an animal model of significantly progressed adenocarcinomas.

Intriguingly, the Pirc rat model shows a significant gender bias in tumor multiplicity and distribution (Table 1). Females are strongly protected from intestinal tumor development and more often become moribund due to the development of jaw tumors and related teeth abnormalities, rather than tumor-related anemia. Women do have a slightly reduced incidence of colorectal cancer compared with men, and recent epidemiologic studies indicate that women have a delayed onset of advanced disease (26, 27). This gender effect may reflect the protective effect of hormones on colon tumor development that has been observed in women on hormone replacement therapy (28).

To have in hand a second experimental mammalian species with which to model human colon cancer creates a new dimension in our ability to understand and manage the disease. By comparing colonic tumors in the human, the mouse, and the rat, we can learn what aspects of the transcriptome, proteome, and biology are species-specific and what aspects are broadly conserved. By comparing autochthonous colonic tumors in the rat with their properties as xenografts in immunodeficient mice, investigators can become more sophisticated at interpreting these two competing experimental platforms when studying the biology, chemoprevention, and therapeutics of human colon cancer.

Materials and Methods

Animal Maintenance. Rats were maintained in standard cages under a university-approved animal protocol in an American Association of Laboratory Animal Care-approved facility. Rats were fed either 5020 chow (Purina, St. Louis, MO) or 8604 chow (Teklad, Madison, WI), with access to an automatic supply of acidified water. Tumor counts were assessed as described with mice in ref. 16, except as noted in Table 2. The following inbred rat strains were used in this study: F344/NTac (Taconic, Hudson, NY) and WF/NHsd (Harlan, Indianapolis, IN).

Colorimetric Yeast Assay. The ENU treatment of male rats for the mutagenesis screen was performed as described in ref. 10. F344 males were injected with 60 mg/kg of ENU once per week for 2 weeks. Long-range PCR from genomic DNA was performed by using the following chimeric universal vector primers: forward, GGC CAT CGA TAG CTC GAT GTA ACG TGC AGT TAA CGC CCA TGT CTC CTG GCT CAA GTT TGC; and reverse, CCT ACT AAC AGA TAC GCT ATG CAG GAC TCT GGA TTG CCC TGT TGG CAT GGC TGA AAT AA. The final PCR concentration mix was 1x Herculase Hotstart buffer (Stratagene, La Jolla, CA), 0.2 mM dNTPs, 25 ng/ul of each primer, 0.15 units/μl Hotstart High-Fidelity DNA Polymerase (Stratagene), 2 μl of genomic DNA, and ddH_2O to 10 μl. PCR conditions were: 94°C for 2 min, then 35 cycles of 94°C for 45 sec, 61°C for 45 sec, and 72°C for 2 min and 30 sec, with a final elongation step of 72°C for 10 min. PCR products were confirmed by gel electrophoresis and cotransformed into yeast along with the universal vector (11).

Genotyping of *Apc*$^{am1137/+}$ Animals. Two PCR amplification methods were developed to genotype the mutant SNP site of the *Apc*^{am1137} allele by restriction enzyme digestion. In one amplicon, the mutant allele was cut by NheI; in the other amplicon, the wild-type allele was cut by HindIII. These complementary methods control for incomplete digestion. The primer sequences were as follows: (for the NheI amplicon) forward, GGA AGA CGA CTA TGA AGA TGG and reverse, TGC CCT GTA CTG ATG GAG; and (for the HindIII amplicon) forward, AAT AAC GTT CAC TGT AGT TGG TAA GCT and reverse, AGG CAA TCA AGA AGC CAG AA.

MicroCT and Endoscopy. Normal chow was replaced with a nonsolid diet the night before microCT imaging. Anesthesia was administered through the regulated flow of isoflurane vapor (1–2%) through a nose cone. The colon was flushed with a warm PBS enema (40 ml). The colon was insufflated with air (20–40 ml), and microCT and endoscopic images were acquired as described below.

Digital Images. Images for Fig. 2 *A–E* and *H* were taken by using automatic exposure with a Spot digital camera (Diagnostic Instruments, Sterling Heights, MI) mounted on a Zeiss (Oberkochen, Germany) Axiophot microscope, with ×2.5, ×20, ×40, ×40, ×5, and ×40 objectives, respectively. Images for Fig. 2 *F*, *G*, *I*, and *J* were taken with a Zeiss Axiocam HRm mounted on a Zeiss Axiovert

200M microscope with ×10, ×63, ×40, and ×40 objectives, respectively, and DAPI and Texas Red filters. Images were taken with Axiovision software (version 4.5.0.0). Fig. 2*F* is a composite of several overlapping images. The microCT image in Fig. 4*A* was acquired on a Siemens (Iselin, NJ) MicroCAT-2 scanner. Acquisition proceeded for 8 min (80 kVp, 500 μA, 400 steps, one frame per view, 360° rotation, 93 × 93 × 100 μm voxel size) and reconstruction was done by using a Shepp–Logan filter with back projection. Amira software (version 4.1; TGS, San Diego, CA) was used for two- and three-dimensional image visualization and media production. Accordingly, isosurface images with appropriate density threshold levels and down-sampled two times along each axis as well as volume-rendered images were created by using the appropriate Amira functions. No further image manipulation was performed. The endoscopy image in Fig. 4*B* was taken with an EG-1870K 6.0-mm color CCD chip video gastroscope and an EPK 1000 video processor (Pentax Medical, Montvale, NJ). The image was captured on the workstation and a hard copy image generated with a Sony Mavigraph video printer (Sony, New York, NY). Fig. 4*C* was photographed with an Olympus (Melville, NY) Camedia C-5050ZOOM digital camera by using automatic exposure.

Somatic ENU Treatment. ENU injection was performed as described in ref. 29.

Immunofluorescence Labeling. Immunofluorescence was performed as described in ref. 30, and images were acquired as described above.

Pyrosequencing Assay. Formalin-fixed tumors were excised under a dissecting microscope to minimize contamination from nontumor tissue. The bottom one-fourth of the polyp, including the muscularis and any surrounding hyperplastic villi were excluded to enrich for tumor regions likely to exhibit Apc loss and β-catenin up-regulation. Excised tissue was incubated overnight in distilled water at 65°C to reverse formalin cross-links. NaOH (100 mM) was added to a final concentration of 50 mM, and samples were incubated at 95°C for at least 4 hours. Tris·HCl (pH 5.5) was then added to neutralize the solution, and the samples were briefly centrifuged. The final PCR mix concentrations were as follows: 1× GoTaq clear buffer, 1.2 mM $MgCl_2$, 0.2 mM dNTP, 264 pM of each primer, 0.6 units of GoTaq Flexi (Promega, Madison, WI), 8 μl of DNA, and ddH_2O to 50 μl. The PCR cycling profile was as follows: 94°C for 3 min, followed by 50 cycles of 94°C for 15 sec, 57°C for 1 min and 30 sec, and 72°C for 2 min, with a final elongation step of 72°C for 10 min. Pyrosequencing assays were performed according to the manufacturer's protocols with Pyro Gold Reagents on a PSQ96MA machine and PSQ 96MA version 2.1 software (Biotage). Forty microliters of PCR product was used per well, and only sequence reads with single base peak heights of >120 units were included. Primer sequences were as follows: (for the Pirc SNP) forward, ATG TGA ACC AGT CTT TGT GTC AG; biotinylated, reverse, ATG CTG TTC TTC CTC AGA ATA ACG; sequencing, GGA AGA CGA CTA TGA AGA T; [for the p arm, SNP (dbSNP ss48531311)], forward, GTG GAA ACG AAG CAT CAT TCT GA; biotinylated, reverse, TGC TGT TCT AAA TTG CAC GTT TAC; sequencing, CGT ATT GGG TTG TGA GA; [for the q arm SNP (dbSNP ss48531727)], biotinylated, forward, TCA AAC AGA AGG CAG TTT ATT CAG; reverse, GGG GGT AAA ATA ATA TGC CGA GA; sequencing, TCT TAG TAA TGT ACC AGA TG. An LOH/maintenance of heterozygosity cutoff value of 32.8% was determined by adapting the normal mixture technique from Shoemaker *et al.* (15) (SI Fig. 5).

Celecoxib Treatment. Rats were treated with 1,200 ppm celecoxib in Teklad 8604 chow given ad libitum, were housed, maintained, and dissected, and their tumors were counted independently of those in Table 1.

We thank Michael Newton for the analysis of LOH data; Linda Clipson for critical reading of the manuscript and assistance with its preparation; Norman Drinkwater, Alexandra Shedlovsky, and Richard Halberg for critical reading; Henry Pitot and Ruth Sullivan for assistance with histopathology; Jane L. Remfert and Yunhong Zan for technical assistance with rat husbandry and yeast screening; and Ben Durkee for assistance with microCT imaging. J.M.A.-L and L.N.K. were supported in part by the National Cancer Institute Institutional Training Grants CA009681 and CA009135, respectively. This work was supported in part by National Institutes of Health Grants CA106216 (to M.N.G.) and CA63677 (to W.F.D.) and by the University of Wisconsin School of Medicine and Public Health. This is publication no. 3633 from the Laboratory of Genetics, University of Wisconsin, Madison.

1. American Cancer Society (2006) *Cancer Facts & Figures 2006* (Am Cancer Soc, Atlanta).
2. Kinzler KW, Vogelstein B (1998) in *The Genetic Basis of Human Cancer*, eds Vogelstein B, Kinzler KW (McGraw–Hill, New York), pp 241–242.
3. Moser AR, Pitot HC, Dove WF (1990) *Science* 247:322–324.
4. Aoki K, Tamai Y, Horiike S, Oshima M, Taketo MM (2003) *Nat Genet* 35:323–330.
5. Sodir NM, Chen X, Park R, Nickel AE, Conti PS, Moats R, Bading JR, Shibata D, Laird PW (2006) *Cancer Res* 66:8430–8438.
6. Dove WF, Clipson L, Gould KA, Luongo C, Marshall DJ, Moser AR, Newton MA, Jacoby RF (1997) *Cancer Res* 57:812–814.
7. O'Brien CA, Pollett A, Gallinger S, Dick JE (2007) *Nature* 445:106–110.
8. Ricci-Vitiani L, Lombardi DG, Pilozzi E, Biffoni M, Todaro M, Peschle C, De Maria R (2007) *Nature* 445:111–115
9. Sjoblom T, Jones S, Wood LD, Parsons DW, Lin J, Barber TD, Mandelker D, Leary RJ, Ptak J, Silliman N, *et al.* (2006) *Science* 314:268–274.
10. Zan Y, Haag JD, Chen KS, Shepel LA, Wigington D, Wang YR, Hu R, Lopez-Guajardo CC, Brose HL, Porter KI, *et al.* (2003) *Nat Biotechnol* 21:645–651.
11. Chen KS, Gould MN (2004) *Biotechniques* 37:383–388.
12. Smits BM, Mudde JB, van de BJ, Verheul M, Olivier J, Homberg J, Guryev V, Cools AR, Ellenbroek BA, Plasterk RH, *et al.* (2006) *Pharmacogenet Genomics* 16:159–169.
13. Smits BM, Guryev V, Zeegers D, Wedekind D, Hedrich HJ, Cuppen E (2005) *BMC Genomics* 6:170.
14. Nordlinger B, Panis Y, Puts JP, Herve JP, Delelo R, Ballet F (1991) *Dis Colon Rectum* 34:658–663.
15. Shoemaker AR, Moser AR, Midgley CA, Clipson L, Newton MA, Dove WF (1998) *Proc Natl Acad Sci USA* 95:10826–10831.
16. Haigis KM, Dove WF (2003) *Nat Genet* 33:33–39.
17. Jacoby RF, Marshall DJ, Newton MA, Novakovic K, Tutsch K, Cole CE, Lubet RA, Kelloff GJ, Verma A, Moser AR, *et al.* (1996) *Cancer Res* 56:710–714.
18. Beazer-Barclay Y, Levy DB, Moser AR, Dove WF, Hamilton SR, Vogelstein B, Kinzler KW (1996) *Carcinogenesis* 17:1757–1760.
19. Jacoby RF, Seibert K, Cole CE, Kelloff G, Lubet RA (2000) *Cancer Res* 60:5040–5044.
20. Corpet DE, Pierre F (2003) *Cancer Epidemiol Biomarkers Prev* 12:391–400.
21. Bulow S, Bjork J, Christensen IJ, Fausa O, Jarvinen H, Moesgaard F, Vasen HF (2004) *Gut* 53:381–386.
22. Schulmann K, Hollerbach S, Kraus K, Willert J, Vogel T, Moslein G, Pox C, Reiser M, Reinacher-Schick A, Schmiegel W (2005) *Am J Gastroenterol* 100:27–37.
23. Pickhardt PJ, Choi JR, Hwang I, Butler JA, Puckett ML, Hildebrandt HA, Wong RK, Nugent PA, Mysliwiec PA, Schindler WR (2003) *N Engl J Med* 349:2191–2200.
24. Gibbs RA, Weinstock GM, Metzker ML, Muzny DM, Sodergren EJ, Scherer S, Scott G, Steffen D, Worley KC, Burch PE, *et al.* (2004) *Nature* 428:493–521.
25. Shisa H, Lu L, Katoh H, Kawarai A, Tanuma J, Matsushima Y, Hiai H (1997) *Mamm Genome* 8:324–327.
26. Jackson-Thompson J, Ahmed F, German RR, Lai SM, Friedman C (2006) *Cancer* 107:1103–1111.
27. Regula J, Rupinski M, Kraszewska E, Polkowski M, Pachlewski J, Orlowska J, Nowacki MP, Butruk E (2006) *N Engl J Med* 355:1863–1872.
28. Rossouw JE, Anderson GL, Prentice RL, LaCroix AZ, Kooperberg C, Stefanick ML, Jackson RD, Beresford SA, Howard BV, Johnson KC *et al.* (2002) *J Am Med Assoc* 288:321–333.
29. Moser AR, Mattes EM, Dove WF, Lindstrom MJ, Haag JD, Gould MN (1993) *Proc Natl Acad Sci USA* 90:8977–8981.
30. Haigis KM, Caya JG, Reichelderfer M, Dove WF (2002) *Proc Natl Acad Sci USA* 99:8927–8931.
31. Corpet DE, Pierre F (2005) *Eur J Cancer* 41:1911–1922.
32. Kohno H, Suzuki R, Yasui Y, Hosokawa M, Miyashita K, Tanaka T (2004) *Cancer Sci* 95:481–486.

Supporting Text

Tumor Phenotype Segregates Perfectly in 56 Carriers and 23 Non-carriers: Suppose the phenotype is due to a linked loci X, r recombination units from Pirc. The Binomial probability of observing no recombinations in 79 trials is 0.046 for r = 0.038 and 0.00969 for r = 0.057.

Consideration of the Possibility That Lethality Is Due to a Second Mutation X: The data taken together strongly support the contention that Pirc is homozygous lethal; however, we have considered the possibility that the lethality is due to a second mutation X linked to Pirc. If X is *r* recombination units from Pirc, the probability of observing a Pirc homozygote at the k^{th} generation, conditional on non-XX parents (P(Pirc/Pirc | non-XX)), is $\frac{0.5\,a_k\left(r - r^2/2\right) + 0.25\,b_k + 0.5\,a_k\,b_k}{0.75\,a_k + b_k + 2\,a_k\,b_k}$ where $a_k = (1-r)^k$ and $b_k = 1 - a_k$.

Using these probabilities, 95% confidence intervals for *r* can be calculated. For example, consider the hypothesis test H0: $r \geq r0$ against HA: $r < r0$. Each value of r0 determines P(Pirc/Pirc | non-XX), the expected proportion of Pirc homozygotes. Using this expected proportion, a Binomial test can be done assuming zero Pirc homozygotes are observed. By inverting the test (1), a conservative 95% confidence interval for *r* is found. When k = 1 and n = 71, the 95% confidence interval for r is (0, 0.0243).

1. Bickel PJ, Doksum KA (2001) *Mathematical Statistics* Vol I, 2nd Ed (Prentice-Hall, New Jersey).

Table 4A. Estimation of gender effect on tumor multiplicity

Tumor class	Gender coefficient	95% Confidence interval	P-value
Colonic adenoma	0.624	0.403, 0.845	< 0.005
Small intestinal adenoma	2.137	1.808, 2.467	< 0.005
Small intestinal microadenoma	1.742	1.639, 1.846	< 0.005

Table 4B. Estimation of age effect on tumor multiplicity

Tumor class	Age coefficient	95% Confidence interval	P-value
Colonic adenoma	0.005	0.004, 0.006	< 0.005
Small intestinal adenoma	0.004	0.003, 0.005	< 0.005
Small intestinal microadenoma	0.006	0.0059, 0.0066	< 0.005

A Poisson regression was used to estimate the effects of gender and age on tumor multiplicity in F344-Pirc animals. The estimated gender (ln of the male/female ratio) and age (ln of the change per day) coefficients are shown. Results show that gender and age significantly affect each phenotype. The results are shown for Poisson regression and were qualitatively similar when a Gaussian regression was used on a square root transformed multiplicity phenotype.

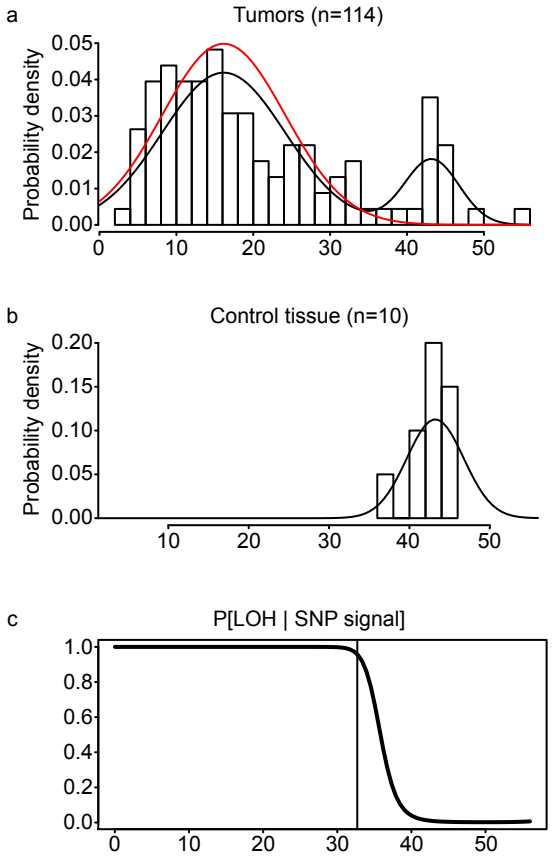

Fig 5. Determination of LOH/maintenance-of-heterozygosity cutoff from pyrosequencing data of tumor and normal Pirc epithelial DNA. We used the method of maximum likelihood to fit a mixture of two normal curves to data on SNP signal intensity. (*a*) Tumor data (n = 114) were considered to arise either from an LOH normal component or a maintenance-of-heterozygosity normal component, according to some mixing probability; (*b*) control data came from a known maintenance-of-heterozygosity component (normal Pirc epithelium n = 10). (*c*) Then, using the fitted mixture model, a critical intensity value c was determined so that Prob[intensity > c | LOH] = .05 . In the estimated normal mixture, the LOH component had mean 16.2 and standard deviation 8.0; the maintenance-of-heterozygosity component had mean 43.2 and standard deviation 3.5; and an estimated fraction 84% of tumors were LOH. From this the critical signal value was c = 32.8. Modes of the likelihood surface at the boundary of the parameter space were avoided. Computations were done in R [R Development Core Team (2005) *R: A language and environment for statistical computing*, http://www.R-project.org].